A SOLVENT-DEPENDENT AND ELECTROCHEMICALLY CONTROLLED SELF-ASSEMBLING/DISASSEMBLING SYSTEM

Valeria AMENDOLA[a1], Massimo BOIOCCHI[b], Yuri DIAZ FERNANDEZ[c], Carlo MANGANO[a2] and Piersandro PALLAVICINI[a3,*]

[a] *Dipartimento di Chimica Generale, Università di Pavia, via Taramelli 12, 27100 Pavia, Italy; e-mail: [1] valeria.amendola@unipv.it, [2] mngcrllf@unipv.it, [3] psp@unipv.it*

[b] *Centro Grandi Strumenti, Università di Pavia, via Bassi 6, 27100 Pavia, Italy; e-mail: massimo@elicona.unipv.it*

[c] *Instituto Superior de Ciencias y de Tecnologias Nucleares, Ave. Salvador Allende y Luaces, Quinta de los Molinos, Plaza de la Ravolucion, Habana, Cuba; e-mail: ydiaz@apache.isctn.edu.cu*

Received May 6, 2003
Accepted August 6, 2003

This paper is dedicated to the outstanding scientific personality of Professor Sergio Roffia, on the occasion of his retirement.

The bis-bidentate ligand *R,S*-1,2-diphenyl-*N,N'*-bis(2-quinolinemethylidene)ethane-1,2-diamine (ligand **4**), containing two (iminomethyl)quinoline moieties separated by a *cis*-1,2-diphenylethylene spacer, forms stable complexes with both Cu^{I} and Cu^{II}. With Cu^{II}, the monomeric 1:1 complex $[Cu^{II}(\mathbf{4})]^{2+}$ is obtained both in CH_3CN and CH_2Cl_2. With Cu^{I} and overall 1:1 metal/ligand molar ratio, an equilibrium mixture is obtained in CH_3CN, consisting of $[Cu^{I}(\mathbf{4})_2]^{+}$, $[Cu^{I}_2(\mathbf{4})_2]^{2+}$ and $[Cu^{I}_2(\mathbf{4})(CH_3CN)_4]^{2+}$. The preponderant species is the two-metal one-ligand "open" complex $[Cu^{I}_2(\mathbf{4})(CH_3CN)_4]^{2+}$, in which each Cu^{+} cation is coordinated in a tetrahedral fashion by one (iminomethyl)quinoline unit and by two CH_3CN molecules. Precipitation from the equilibrium mixture yields only crystals of $[Cu^{I}_2(\mathbf{4})(CH_3CN)_4](ClO_4)_2 \cdot 2CH_3CN$, whose crystal and molecular structures have been determined. On the other hand, in the poorly coordinating CH_2Cl_2 solvent, only the dimeric helical $[Cu^{I}_2(\mathbf{4})_2]^{2+}$ complex is obtained, when the overall metal/ligand 1:1 molar ratio is chosen. Addition of large quantities of acetonitrile to solutions of $[Cu^{I}_2(\mathbf{4})_2]^{2+}$ in dichlorometane results in the formation of $[Cu^{I}_2(\mathbf{4})(CH_3CN)_4]^{2+}$, *i.e.* in the solvent-driven disassembling of the Cu^{I} helicate. While electrochemistry in CH_3CN is poorly defined due to the presence of more than one Cu^{I} species, cyclic voltammetry experiments carried out in CH_2Cl_2 revealed a well defined behavior, with irreversible oxidation of $[Cu^{I}_2(\mathbf{4})_2]^{2+}$ and irreversible reduction of $[Cu^{II}(\mathbf{4})]^{2+}$ taking place at separate potentials ($\Delta E \approx 700$ mV). Irreversibility and separation of the redox events are due to the self-assembling and disassembling processes following the reduction and oxidation, respectively.

Keywords: Helical structures; Electrochemistry; Molecular machines; Copper complexes; Imine ligands; Nitriles; Salenes; Quinolines; Chiral ligands; Cyclic voltammetry.

The possibility of controlling the movement of a part of a molecular system or of controlling the overall rearrangement between two or more possible conformations of large molecules have been subject of interest in recent years, introducing to the field of molecular machines[1]. The external input which gives origin to the movements can be either of chemical nature (*e.g.* pH)[2] or of photochemical nature[3] even though it appears to be particularly advantageous and sharply working when it is a change in the applied potential, *i.e.* when the input is of electrochemical[4] nature.

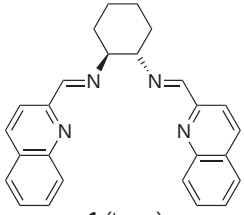

1 (trans)

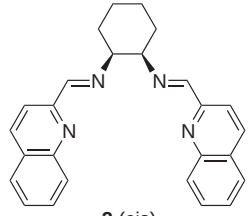

2 (cis)

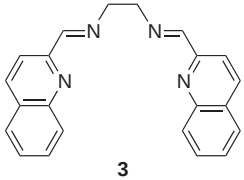

3

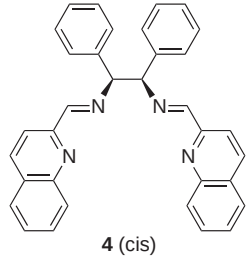

4 (cis)

Systems capable of electrochemically controlled self-assembling/disassembling of metal helicates have been known since the beginnings of supramolecular chemistry and are indeed coeval with the development of the concept of metal helicates[5]. We recently contributed to this field by publishing a series of papers in which we presented a series of ligand/metal systems capable of undergoing electrochemically controlled self-assembling/disassembling of helical structures[6]. In these systems, a bis-bidentate (iminomethyl)-heterocycle ligand (*e.g.* L = **1**–**3**) forms a monomeric complex with Cu^{2+}, $[Cu^{II}(L)]^{2+}$ (form **c** in Scheme 1), in a square arrangement, due to the preferences to elongated octahedral coordination of d^9 cations. On the other hand, the same ligand is not capable of folding and arranging around a d^{10} Cu^{+} cation according to the preferred tetrahedral disposition. Accordingly, a 2:2 metal/ligand helical complex is obtained, $[Cu^{I}_2(L)_2]^{2+}$ (form **a** in Scheme 1). The interesting features of these systems are that the transition

between the forms can be both observed electrochemically (by cyclic voltammetry) and carried out in a bulk solution (by controlled potential coulometry). The transformations between $[Cu^{II}(L)]^{2+}$ and $[Cu^{I}_2(L)_2]^{2+}$ appear irreversible on the CV profile, due to the fast rearrangements following the oxidation and reduction processes, *i.e.* disassembling and self-assembling. Scheme 1, which is a typical example of a "square scheme"[7] made by the combination of two EC processes[8] illustrates which are the redox and chemical processes involved (Scheme 1 is drawn for ligand **4**, but identical schemes can be drawn for **1**–**3**).

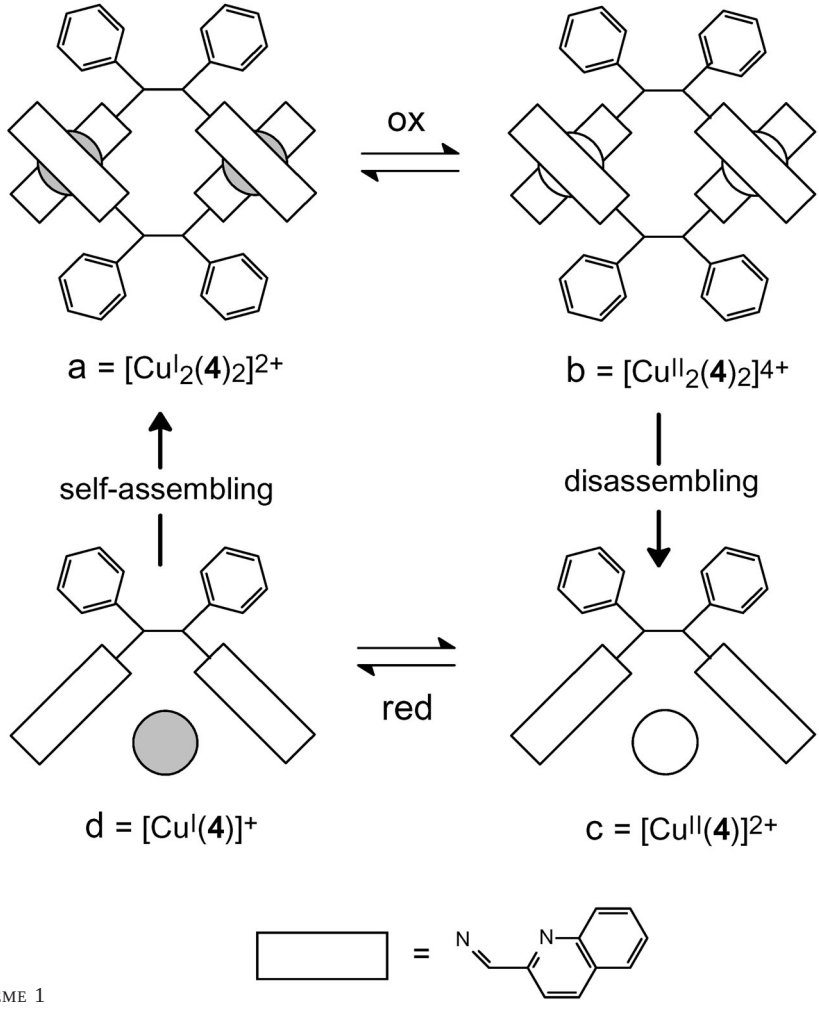

SCHEME 1

However, reversibility of the electrochemical transformation between monomeric $[Cu^{II}(L)]^{2+}$ and helical dimeric $[Cu^{I}_2(L)_2]^{2+}$ is complete, as demonstrated by repeated CPC cycling. In addition, these systems appear particularly fast in the rearrangement processes following the electrochemical ones, the former being complete in less than 20 ms [6b]. Moreover, due to the energy expenses necessary to the rearrangements taking place after the redox events[9], the oxidation and reduction processes are well separated (600–1000 mV) so that these systems display electrochemical hysteresis.

The spacer between the two (iminomethyl)-heterocycle moieties is the part of ligands of the **1**–**3** type that can be easily subject to further functionalization, *e.g.* with groups apt for coordination to an external metal cation or for grafting on a surface. However, the bulkness of the substituents on the spacer may influence the capability of the ligands to form metal helicates, which are molecules in which the volume/mass ratio is minimized[10]. In this perspective, we have examined the solution and redox behavior of the Cu^{I} and Cu^{II} complexes of ligand **4**, which has the same framework as ligand **3** but bears two bulky phenyl groups in *R,S-* (“*cis-*”) disposition on the ethylene spacer. Interestingly, while Cu^{II} complexes are monomeric as expected, the bulkiness of the substituents introduces a serious effect on the structure assumed by the Cu^{I} complexes. Only in a poorly coordinating solvent such as CH_2Cl_2 the $[Cu^{I}_2(\mathbf{4})_2]^{2+}$ helicate is obtained and the electrochemical behavior depicted in Scheme 1 occurs. In CH_3CN, a solvent which has strong affinity to Cu^{I}, the system prefers to open, forming monoligand-dimetallic species, thanks to the coordination of acetonitrile molecules to the copper(I) centres: in this case the electrochemical behavior is less defined and the system does not present an hysteresis profile.

RESULTS AND DISCUSSION

Solvent Dependence on the Formation of Cu^{I} Helicates

On the basis of the results found for ligands **1**–**3**, the ability of ligand **4** to form Cu^{I} helicates was first checked in acetonitrile by titration of the ligand with substoichiometric quantities of $[Cu^{I}(CH_3CN)_4]ClO_4$. Beginning from the first additions, the solution took a violet color, with growing intense band centered at 545 nm, resembling the typical MLCT band originating by the interaction of two (iminomethyl)quinoline ligands with Cu^{I}. This band can be compared with that observed for the helicates $[Cu^{I}_2(L)_2]^{2+}$ with ligands **1**–**3**, which showed absorption maxima at 536, 543 and 535 nm. Inter-

estingly, in the case of **1**–**3**, following the profile of the absorbance at λ_{max} *vs* added metal ion, a more or less pronounced inflection was found at 0.5 equivalents, corresponding to the formation of a significant quantity of a 2:1 ligand/metal complex, $[Cu^{I}(L)_2]^+$ but, after that point, absorbance continued to grow up to 1.0 equivalent of added metal, after which value a straight plateau was observed[6]. This corresponded to the formation of very stable complexes of apparent 1:1 stoichiometry, which indeed were the 2:2 helicates $[Cu^{I}_2(L)_2]^{2+}$. In the case of ligand **4**, the band centered at λ_{max} = 545 nm grows up to 0.5 equivalent of added Cu^+ but, on further addition of metal, its intensity decreases, while a new band, centered at 416 nm begins to form, with the solution changing color from violet to red. The profiles of the variations in the intensity of the two bands show a smooth inflection at 1.0 equivalent while and endpoint is observed at 2.0 equivalents of added Cu^+. Figure 1 reports the series of spectra obtained by addition of Cu^+ to ligand **4**, while the inset displays the profile of the absorbance at 545 and 416 nm *vs* equivalent of Cu^+.

These data imply that in addition to the formation of a $[Cu^{I}(\mathbf{4})_2]^+$ species, only small quantites of $[Cu^{I}_2(\mathbf{4})_2]^{2+}$ are formed, while the most stable species found in solution for metal/ligand stoichiometries around 1 or higher is the 2:1 complex $[Cu^{I}_2(\mathbf{4})]^{2+}$ (for which, on the basis of the final spectra and on the used ligand concentration, an ε value of 4680 l mol^{-1} cm^{-1} for the 416 nm band can be calculated). This is confirmed also by the X-ray crystal structure determined on crystals precipitated from a solution con-

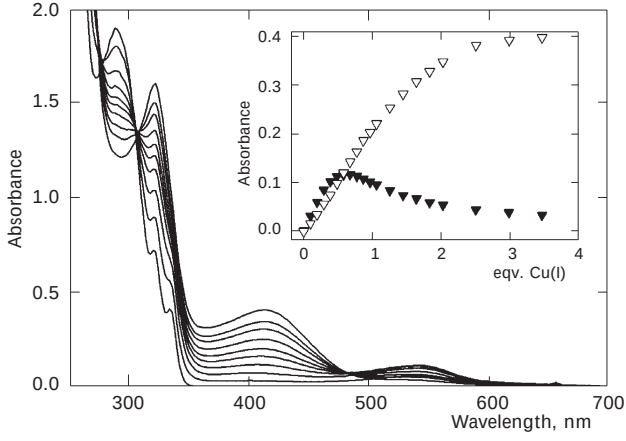

FIG. 1
Series of spectra obtained by addition of substoichiometric quantities of Cu^+ to ligand **4** in acetonitrile. The inset displays the absorbance *vs* equivalents of added Cu^+ at 516 (▼) and 416 (▽) nm

taining Cu^I and ligand **4** in a molar ratio 1:1 a complex is obtained in which ligand **4** is open and hosts one Cu^+ cation for each (iminomethyl)-quinoline bidentate unit, with two acetonitrile molecules completing the tetrahedral coordination sphere of each copper atom (see Fig. 4 and following paragraph for detailed discussion). Accordingly, the dimetallic complex is better formulated as $[Cu^I_2(\mathbf{4})(CH_3CN)_4]^{2+}$ (form e in Scheme 2). Interestingly, this seems another example of one product crystallizing out of a dynamic equilibrium mixture[11]: the ^1H NMR spectrum of a CD_3CN solution of Cu^+ and ligand **4** (1:1) displays a complicated and poorly resolved pattern at 20 °C, which does not simplify by changing the temperature to higher or lower values, while the ESI mass spectrum clearly shows a preponderance of the $[Cu^I_2(\mathbf{4})]^{2+}$ molecular cation (*m/z* = 715, 717, 719 for $\{[Cu^I_2(\mathbf{4})](ClO_4\}^+$: the loosely bound acetonitrile molecules are lost during ionization) and the formation of only a small quantity of the helical dimer $[Cu^I_2(\mathbf{4})_2]^{2+}$ (*m/z* = 1205, 1207, 1208, 1210 for $\{[Cu^I_2(\mathbf{4})_2](ClO_4\}^+$)[12]. The reason for the prevalent formation of the "open" complex $[Cu^I_2(\mathbf{4})(CH_3CN)_4]^{2+}$ with respect to $[Cu^I_2(\mathbf{4})_2]^{2+}$ seems to consist both in the difficulties found by the two ligands to intertwin around two metals to form a helicate and in the affinity of the nitrile molecules to Cu^+. Molecular modelling[13] (Fig. 2), while suggesting that for the $[Cu^I_2(\mathbf{4})_2]^{2+}$ species the helical form is more stable than the side-by-side form, evidences crowding in the molecular cation. In particular, each phenyl ring of the first ligand lies in close proximity to one quinoline ring of the second ligand.

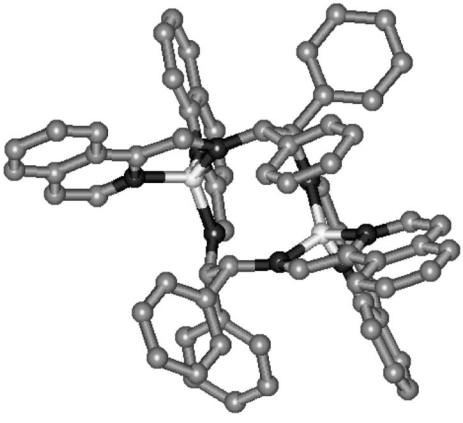

FIG. 2
Molecular model for the helical $[Cu^I_2(\mathbf{4})_2]^{2+}$ dimer obtained in dichloromethane (carbon atoms grey, nitrogen atoms black, copper atoms shaded white)

On the other hand, a titration of ligand **4** dissolved in non-coordinating solvent CH_2Cl_2 by addition of microquantities of $[Cu^I(CH_3CN)_4]ClO_4$ dissolved in acetonitrile evidenced the formation only of the 2:2 species, with the growth of the expected band at 544 nm (ε = 6000) and a titration profile A_{544} *vs* amount of Cu^+ evidencing a sharp change at 1.0 equivalent of added metal, as shown in Fig. 3.

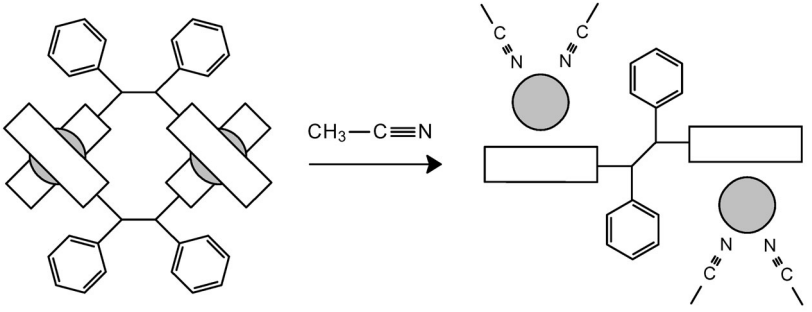

SCHEME 2

Further confirmation of the formation of the helical $[Cu^I_2(\mathbf{4})_2]^{2+}$ complex in CH_2Cl_2 comes from mass spectra measurements (ESI) carried out on solutions of ligand **4** and Cu^+ in molar ratio 1:1, in which the only dimeric species found displays the expected 1205, 1207, 1208, 1210 *m/z* set of values,

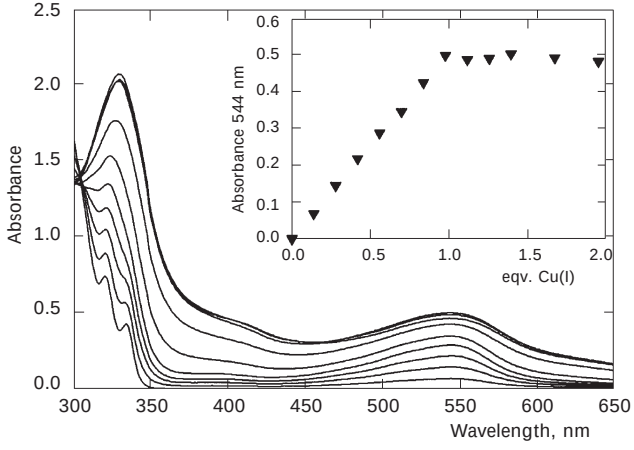

FIG. 3

Series of spectra obtained by addition of substoichiometric quantities of Cu^+ to ligand **4** in dichloromethane. The inset displays the absorbance *vs* equivalents of added Cu^+ at 544 nm

corresponding to the $\{[Cu^{I}_2(\mathbf{4})_2](ClO_4)\}^+$ molecular cation. Accordingly, the preferred formation of the helical dimer in CH_2Cl_2 can be justified by the absence of significant quantities of the coordinating CH_3CN solvent. Interestingly, addition of increasing quantites of acetonitrile to a dichloromethane solution of $[Cu^{I}_2(\mathbf{4})_2]^{2+}$ (ref.[14]) resulted in a decrease in the 544 nm band and an increase in the 416 nm band, relative to the "open" $[Cu^{I}_2(\mathbf{4})(CH_3CN)_4]^{2+}$ complex[15]. Accordingly, as depicted in Scheme 2, the disassembling process of the Cu^{I} helicate can be controlled by changing the solvent composition, in a new example of systems related to "molecular machines" in which it is the solvent making the system state change[16].

Crystal and Molecular Structure of $[Cu^{I}_2(\mathbf{4})(CH_3CN)_4](ClO_4)_2 \cdot 2CH_3CN$

The red crystals on which X-ray diffraction has been carried out were obtained by slow diffusion of diethyl ether in an acetonitrile solution of ligand **4** and $[Cu^{I}(CH_3CN)_4]ClO_4$ (molar ratio 1:1). This means that $[Cu^{I}_2(\mathbf{4})(CH_3CN)_4](ClO_4)_2 \cdot 2CH_3CN$ is the most stable form in the solid state out of a series of species which undergo dynamic equilibrium in solution. The structure of the $[Cu^{I}_2(\mathbf{4})(CH_3CN)_4]^{2+}$ molecular cation is shown in Fig. 4.

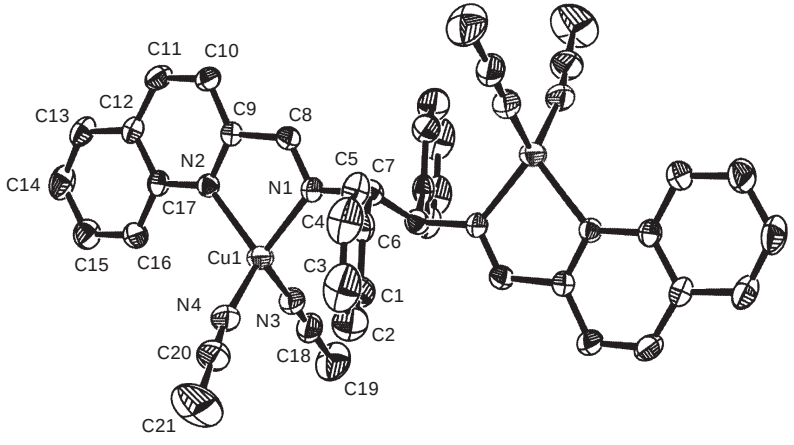

FIG. 4

Ortep diagram of the $[Cu^{I}_2(\mathbf{4})(CH_3CN)_4]^{2+}$ complex. Thermal ellipsoids are drawn at the 30% probability level. Hydrogen atoms, ClO_4^- counter-anions and non-coordinating CH_3CN groups are omitted for clarity. Selected bond distances (in Å) and angles (in °). Cu1–N1 2.065(3), Cu1–N2 2.073(3), Cu1–N3 1.942(4), Cu1–N4 1.964(4); N1–Cu1–N2 80.2(1), N1–Cu1–N3 118.6(2), N1–Cu1–N4 115.9(2), N2–Cu1–N3 115.2(1), N2–Cu1–N4 117.7(1), N3–Cu1–N4 107.6(2). Cu–Cu distance 6.668(2) Å

In addition to the release of the crowding expected for the 2:2 helical form and the affinity of the Cu^+ cation to the acetonitrile ligand, the formation of this species can be favored by the extended π–π stacking interactions found in the crystal. In particular, each benzene and quinoline ring in one complex molecule is parallel to benzene and quinoline rings in different molecules. The shortest C–C distances between π–π stacked benzene rings are in the range of 3.637–3.709 Å, while between parallel quinoline rings the shortest N–C distances are 3.563 and 3.653 Å, the shortest C–C distances being in the range of 3.608–3.649 Å. Each molecule of the complex cation $[Cu^I_2(\mathbf{4})(CH_3CN)_4]^{2+}$ is thus surrounded by four other independent molecules, thus forming molecular layers lying in the (010) plane. From both sides of each layer depart the CH_3CN ligands bonded to Cu^I atoms and between two parallel layers is a layer containing the ClO_4^- anions and isolated CH_3CN ligands, thus allowing the formations of weak C–H···O interactions and van der Waals forces that stabilize the crystal along *b* axis.

The asymmetric unit corresponds to half of the formula unit, due to a point of inversion which lies in the midpoint of the C7–C7′ bond. The asymmetric unit is also a complete and neutral half of the complex: it contains an (iminomethyl)quinoline and the adjacent phenyl group, the Cu^+ atom coordinated by the two nitrogen atoms of the (iminomethyl)quinoline group and by the two nitrogen atoms of two CH_3CN moelcules, plus an isolated ClO_4^- anion and an isolated CH_3CN molecule. Accordingly, the geometrical features between the two halves of a $[Cu^I_2(\mathbf{4})(CH_3CN)_4]^{2+}$ molecule are constrained by the inversion point and the two quinoline planes or the two benzene planes are parallel. The Cu^+ atoms show a distorted tetrahedral coordination. The longest bonds occur with the nitrogen atoms of the ligand (Fig. 4), for which also the smallest N–Cu–N bond angle is measured. The (iminomethyl)quinoline part of the ligand and the coordinated Cu^+ atom are almost perfectly coplanar, with Cu^+ deviating from the (iminomethyl)quinoline mean least-square plane of 0.013(3) Å. The observed bond distances and angle with the nitrogen atoms of the ligand are similar with those found for the Cu^+ helical complexes of ligands **1** and **2** (ref.[6]), where Cu^+ shows anyway a more distorted tetrahedral coordination. No direct interaction occurs between Cu^I and the anions (shortest Cu–O distance is 4.644(15) Å), and the Cu^I–Cu^I distance between the cations of the complex is 6.668(2) Å. Phenyl, quinoline and imine groups show regular bond distances and angles. The angle between the benzene and the (iminomethyl)quinoline mean least-square plane in the asymmetric unit is 68.9(1)°.

Electrochemically Driven Self-Assembling/Disassembling of Helicates

Prior to electrochemical measurements, the monomeric nature of the Cu^{II} complex with ligand **4** has been verified. Spectrophotometric titrations were carried out in CH_3CN and CH_2Cl_2 by addition of substoichiometric quantities of $Cu^{II}(CF_3SO_3)_2$ to ligand **4**, observing the formation of a typical d-d band (λ_{max} = 700 nm, ε = 140 l mol^{-1} cm^{-1} in both solvents), already found in the case of **1**–**3** (λ_{max} = 668, 672 and 677 nm and ε = 105, 150 and 200 l mol^{-1} cm^{-1}, respectively[6]). The A_{700} *vs* equivalent of Cu^{2+} profile gave the expected sharp inflection at 1:1 stoichiometry, but addition of excess Cu^{2+} resulted in further minor variations of the d-d band. This indicates that the 1:1 complex is particularly stable but that in the presence of excess Cu^{2+} the ligand tends to open and coordinate (at least in part) the excess metal cation, to form $[Cu^{II}_2(\mathbf{4})]^{4+}$. However, mass spectra (ESI) on solutions of copper(II) triflate and ligand **4** (molar ratio 1:1) gave a signal at *m/z* = 702, corresponding to $\{[Cu^{II}(\mathbf{4})](CF_3SO_3)\}^+$, confirming the preference for this species when the correct stoichiometry is chosen.

Cyclic voltammetry experiments were first carried out in acetonitrile on solutions of Cu^+/ligand **4** (1:1). Under these conditions, separate and irreversible oxidation and reduction signals were observed. However, differently from what was found for the copper complexes of ligands **1**–**3** and while a well defined irreversible reduction is found (E_{red} = –100 mV *vs* Fc^+/Fc), a flat irreversible wave is observed in oxidation, extended to the 600–800 mV *vs* Fc^+/Fc range (Fig. 5a, dotted curve).

This can be attributed to the presence of the dynamic equilibrium among the $[Cu^I(\mathbf{4})_2]^+$, $[Cu^I_2(\mathbf{4})_2]^{2+}$ and $[Cu^I_2(\mathbf{4})(CH_3CN)_4]^{2+}$ species to which the 1:1 ligand/Cu^+ mixture is subject, so that a mixture of three different species is oxidized. On the other hand, reduction takes place from only one Cu^{II} species, $[Cu^{II}(\mathbf{4})]^{2+}$, which is the preferred one at the ligand **4**/Cu^{2+} 1:1 molar ratio. Examination of the CV profile of a solution containing ligand **4**/Cu^+ in molar ratio 1:2 revealed a different behavior (Fig. 5a, solid line). Also in this case, only irreversible redox processes are observed, but while a sharper oxidation occurs at higher potentials (≈800 mV *vs* Fc^+/Fc), two distinct reduction waves are found, one centered at 410 and the second centered at –100 mV *vs* Fc^+/Fc. In this case, the oxidation process can be attributed to the simultaneous oxidation of the Cu^+ centres in only one species, $[Cu^I_2(\mathbf{4})]^{2+}$ (in which, according to the crystal structure, the two copper centres are well separated, as they lie at 6.668 Å distance), while on oxidation, due to the presence of two Cu^{2+} cations for each ligand, the system undergoes redistribution to a mixture of $[Cu^{II}(\mathbf{4})]^{2+}$ and $[Cu^{II}_2(\mathbf{4})]^{4+}$, from which

two different reduction processes take place. Thus, due to the presence of more than one species in dynamic equilibrium at both 1:1 and 1:2 ligand/metal ratios, the behavior of the copper/**4** system is not straightforward in acetonitrile, and in particular it is differrent from what was described for ligands **1**–**3**.

On the other hand, in CH_2Cl_2 only two forms are present for the system if 1:1 ligand/metal stoichiometry is considered: $[Cu^{II}(\mathbf{4})_2]^{2+}$ and $[Cu^{I}{}_2(\mathbf{4})_2]^{2+}$.

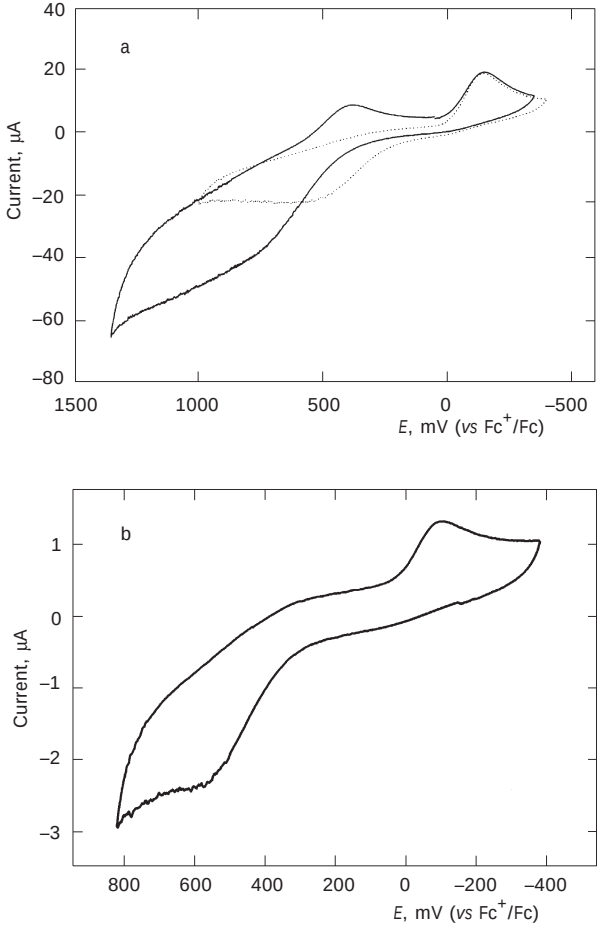

FIG. 5

Cyclic voltammetry profile obtained: **a** in acetonitrile (0.1 M tetrabutylammonium perchlorate, scan rate 200 mV s^{-1}) for the 1:1 ligand **4**/Cu^+ stoichiometry (dotted line) and for the 1:2 ligand **4**/Cu^+ stoichiometry (solid line); **b** in dichloromethane (0.1 M tetrabutylammonium perchlorate, scan rate 200 mV s^{-1}) for the 1:1 ligand **4**/Cu^+ stoichiometry

Accordingly, CV measurements (Fig. 5b) revealed the typical profile already found for **1**–**3** when measured in dichloromethane solutions of **4** with either Cu^+ or Cu^{2+} (1:1): an irreversible wave is observed at –110 mV *vs* Fc^+/Fc, due to the reduction of the monomeric $[Cu^{II}(\mathbf{4})_2]^{2+}$ complex (followed by self-assembling to the helical dimer $[Cu^{I}_2(\mathbf{4})_2]^{2+}$), and a separated irreversible wave is observed at +580 mV *vs* Fc^+/Fc, due to the oxidation of the helical dimer $[Cu^{I}_2(\mathbf{4})_2]^{2+}$ (followed by disassembling to the monomer $[Cu^{II}(\mathbf{4})_2]^{2+}$).

According to these data, also this system displays electrochemical hysteresis, and Scheme 1a holds. Interestingly, the observed potential values are different from those reported for the closely related ligand **3** (E_{ox} = 692, E_{red} = –10 mV *vs* Fc^+/Fc). The separation between the oxidation and reduction is similar (ΔE = 700 mV) but a shift of the potentials of both events is observed towards lower values, similarly to what was found with ligand **2** (E_{ox} = 430, E_{red} = –250 mV *vs* Fc^+/Fc), in which, significantly, the (iminomethyl)quinoline bidentate units are appended to a cyclohexane spacer in *cis* arrengement, as in ligand **4**.

EXPERIMENTAL

Synthesis

R,*S*-1,2-Diphenylethane-1,2-diamine and quinoline-2-carbaldehyde have been purchased from Sigma–Aldrich and used without further purification.

R,S-1,2-Diphenyl-N,N′-bis(2-quinolinemethylidene)ethane-1,2-diamine (**4**). *R*,*S*-1,2-Diphenylethane-1,2-diamine (0.212 g, 1.00 mmol) and quinoline-2-carbaldehyde (0.314 g, 2.00 mmol) were dissolved in 30 ml CH_2Cl_2. The obtained solution was stirred at room temperature and under nitrogen for 16 h, after which time a yellowish precipitate of ligand **4** was obtained. The product was separated by suction and washed with 5 ml of cold diethyl ether. The dichloromethane solution was concentrated to 10 ml on a rotary evaporator, thus obtaining further solid product, which was filtered, washed with 5 ml of cold diethyl ether and combined with the first batch. Total yield 76%. For $C_{34}H_{26}N_4$ (490.6) calculated: 83.28% C, 5.30% H, 11.42% N; found: 83.11% C, 5.21% H, 11.34% N. ^{1}H NMR ($CDCl_3$): 8.37 (s, 2 H, imine -CH=N-); 8.27 (d, 2 H) + 8.21 (d, 2 H) + 8.10 (d, 2 H) + 7.88 (d, 2 H) + 7,76 (t, 2 H) + 7.61 (t, 2 H) + 7.54 (d, 4 H) + 7.32 (t, 4 H) + 7.21 (t, 2 H), H of the benzene and quinoline rings; 5.08 (s, 2 H, CH-CH of the ethylene spacer). ESI MS, *m/z*: 491 {**4** + H}$^+$.

$[Cu^{I}_2$(R,S-1,2-diphenyl-N,N′-bis(2-quinolinemethylidene)ethane-1,2-diamine)$(CH_3CN)_4](ClO_4)_2 \cdot 2CH_3CN$, *$[Cu^{I}_2(\mathbf{4})(CH_3CN)_4](ClO_4)_2 \cdot 2CH_3CN$*. Ligand **4** (20.0 mg, 0.041 mmol) and $[Cu(CH_3CN)_4]ClO_4$ (13.4 mg, 0.041 mmol) were dissolved in 5.0 ml of CH_3CN, and Et_2O was allowed to slowly diffuse into this solution. The product was obtained after 4 days as red crystals. Separation by decantation and immediate sealing of some crystals in a capillary with the mother liquor allowed to obtain samples suitable for X-ray diffraction experiments. The remaining batch was separated by suction filtration and dried in a desiccator: after few minutes the product lost its crystalline appearance, due to the loss of non-coordinating ace-

tonitrile, giving a red powder (yield 27%), which was not stable enough to allow CHN analysis (oxidation to greenish Cu^{II} products was observed within few hours). The freshly prepared red product was used to obtain ESI MS (acetonitrile), *m/z*: 715, 717, 719 $\{[Cu^{I}_2(\mathbf{4})](ClO_4)\}^+$.

$[Cu^{I}_2$(R,S-1,2-Diphenyl-N,N′-bis(2-quinolinemethylidene)ethane-1,2-diamine)$_2](ClO_4)_2 \cdot CH_2Cl_2$, $[Cu^{I}_2(\mathbf{4})_2](ClO_4)_2 \cdot CH_2Cl_2$. Ligand **4** (20.0 mg, 0.041 mmol) was dissolved in 50 ml of dichloromethane and treated with 13.4 mg (0.041 mmol) of $[Cu(CH_3CN)_4]ClO_4$, dissolved in 0.5 ml of hot acetonitrile. The solution immediately took a deep violet color and after 20 min the product precipitated as a fine violet powder. Further precipitate was obtained by reducing the volume of the reaction mixture to 30 ml on a rotary evaporator. The product was separated by suction, washed with 5 ml of Et_2O and dried in vacuum. Any attempt to obtain crystals by slow ether diffusion into the dichloromethane solution was unsuccessfull. Yield 65%. For $C_{69}H_{54}Cu_2Cl_4N_8O_8$ (1392.1) calculated: 59.56% C, 3.88% H, 8.05% N; found: 59.47% C, 3.81% H, 7.99% N. ESI MS (CH_2Cl_2), *m/z*: 1205, 1207, 1208, 1210 $\{[Cu^{I}_2(\mathbf{4})_2](ClO_4)\}^+$.

Instrumentation

UV/VIS spectra were taken on a Hewlett–Packard HP8453 diode array spectrophotometer. IR spectra were obtained on a Mattson 5000-FT-IR instrument. ^{1}H NMR spectra with a Bruker AMX 400 spectrometer. Mass spectra (ESI) were recorded on a Finnigan MAT TSQ 700 instrument.

Electrochemical Measurements

Cyclic voltammetry studies were carried out in anhydrous 0.1 M CH_3CN or CH_2Cl_2 solutions in $(t\text{-}Bu_4N)ClO_4$. Concentration of the electroactive species was in the 10^{-3}–10^{-4} mol l^{-1} range. Scan speed was 200 mV s^{-1}. Faster scan speeds have also been used to check if return waves could be observed, however, up to 2000 mV s^{-1} no return waves were observed (in faster scan speeds the profiles lost resolution). The working electrode was a platinum microsphere and the counter electrode a platinum wire. The potential values were determined by using a platinum wire as the reference electrode and by adding ferrocene to the working solution as an internal standard.

Spectrophotometric Titrations

In a typical experiment, ligand **4** was dissolved in 40–50 ml of acetonitrile or dichloromethane to obtain 1–8 × 10^{-4} M solutions. Compounds $Cu(CF_3SO_3)_2$ or $[Cu^{I}(CH_3CN)_4]ClO_4$ dissolved in acetonitrile were added as solutions of such a concentration that a 1:1 ligand/metal stoichiometry was reached with a 200 µl addition. In a typical titration, 15–30 additions of 10–20 µl each were made, using a 1-mm quartz cell and a 1-cm quartz cell for the titrations with Cu^{I} and Cu^{II}, respectively.

X-Ray Crystal Structure Determination

Single-crystal X-ray diffraction data (graphite-monochromatized MoKα radiation) were collected for a prismatic red crystal by using a Bruker–Axs three-circle diffractometer equipped with a Smart–Apex two-dimensional CCD detector. Crystallographic data are presented in Table I. Crystals of the complex $[Cu^{I}_2(\mathbf{4})(CH_3CN)_4](ClO_4)_2 \cdot 2CH_3CN$ placed in air decayed in

about 15 min, hence X-ray data collection was performed for a single crystal placed in a closed glass capillary containing a small amount of mother liquor. An amount of 600 frames was collected (omega-scan of 0.3° and acquisition time of 20 s) using the Smart software (Bruker–Axs Inc) at ϕ = 0, 120, and finally 240°. After 11 h 1800 frames were processed with the Saint software (Bruker–Axs Inc) and the intensities of 11 522 reflections were integrated. Unit-cell parameters were obtained by least-square refinement of 2250 reflections of $F_o > 10\sigma(F_o)$ and $1 \le \theta \le 11$. An empirical absorption correction was applied at the integrated intensities[17]. The structure was solved by direct method (SIR97)[18] in the $P\bar{1}$ space group

TABLE I
Crystallographic data, data collection and structure refinement for $[Cu^{I}_2(\mathbf{4})(CH_3CN)_4](ClO_4)_2 \cdot 2CH_3CN$

Formula	$C_{46}H_{44}Cl_2Cu_2N_{10}O_8$
M, g mol^{-1}	1062.89
Crystal size, mm^3	0.28 × 0.22 × 0.14
Crystal description	prism
T, K	293
Crystal system, space group	triclinic; $P\bar{1}$ (No.2)
a, Å; α, °	9.267(3); 75.90(1)
b, Å; β, °	12.218(4); 73.91(1)
c, Å; γ, °	12.201(4); 73.55(1)
V, Å^3; Z	1252.4(8); 1
D_c, g cm^{-3}	1.409
F(000); μ(MoKα), mm^{-1}	546; 1.02
θ range, deg; data completeness, %	1.8–26.2; 0.99
hkl range	–11/11; –15/15; –15/14
No. of integrated diffractions	11 522
No. of unique diffractions	4976
R_{int}[a], %	4.38
No. of diffractions with $F_o \ge 2\sigma(F_o)$	2964
No. of parameters	320
R; wR for all data[b], %	10.07; 17.04
R; wR for diffractions with $F_o \ge 2\sigma(F_o)$[b]	5.39; 14.47
GOF for all data[c]	0.942
Residual electron density, e Å^{-3}	0.59; –0.34

[a] $R_{int} = \Sigma|F_o^2 - \langle F_o^2\rangle|/\Sigma F_o^2$. [b] $R(F) = \Sigma||F_o| - |F_c||/\Sigma|F_o|$, $wR(F^2) = [\Sigma(w(F_o^2 - F_c^2)^2)/\Sigma(w(F_o^2)^2)]^{1/2}$. [c] GOF = $[\Sigma(w(F_o^2 - F_c^2)^2)/(N_{diffrs} - N_{params})]^{1/2}$.

and refined by full-matrix least-square procedure on F^2 using all reflections (SHELXl97)[19]. Non-hydrogen atoms were refined anisotropically; hydrogen atoms were identified in the ΔF maps and isotropically refined with the appropriate AFIX instruction.

CCDC 208736 contains the supplementary crystallographic data for this paper. These data can be obtained free of charge *via* www.ccdc.cam.ac.uk/conts/retrieving.html (or from the Cambridge Crystallographic Data Centre, 12, Union Road, Cambridge, CB2 1EZ, UK; fax: +44 1223 336033; or deposit@ccdc.cam.ac.uk).

This work has been supported by the EU (RT Network Molecular Level Devices and Machines, contract HPRN-CT-2000-00029) and by the University of Pavia (FAR).

REFERENCES AND NOTES

1. Balzani V., Credi A., Raymo F. M., Stoddart J. F.: *Angew. Chem.* **2000**, *39*, 3348.
2. Amendola V., Fabbrizzi L., Mangano C., Pallavicini P.: *Acc. Chem. Res.* **2001**, *34*, 488.
3. a) Benniston A. C., Harriman A.: *Angew. Chem., Int. Ed. Engl.* **1993**, *32*, 1459; b) Benniston A. C., Harriman A., Lynch V. M.: *Tetrahedron Lett.* **1994**, *35*, 1473; c) Ashton P. R., Ballardini R., Balzani V., Credi A., Dress R., Ishow E., Kleverlaan C. J., Kocian O., Preece J. A., Spencer N., Stoddart J. F., Venturi M., Wenger S.: *Chem. Eur. J.* **2000**, *6*, 3558.
4. a) Raehm L., Kern J.-M., Sauvage J.-P.: *Chem. Eur. J.* **1999**, *5*, 3310; b) Armaroli N., Balzani V., Collin J.-P., Gavina P., Sauvage J.-P., Ventura B.: *J. Am. Chem. Soc.* **1999**, *121*, 4397; c) Ballardini R., Balzani V., Dehaen W., Dell'Erba A. E., Raymo F. M., Stoddart J. F., Venturi M.: *Eur. J. Org. Chem.* **1999**, 591; d) Ceroni P., Leigh D. A., Mottier L., Paolucci F., Roffia S., Tetard D., Zerbetto F.: *J. Phys. Chem. B* **1999**, *103*, 10171; e) Cardenas D. J., Livoreil A., Sauvage J.-P.: *J. Am. Chem. Soc.* **1996**, *118*, 11980.
5. Gisselbrecht J.-P., Gross M., Lehn J.-M., Sauvage J.-P., Ziessel R., Piccinni-Leopardi C., Arrieta J. M., Germain G., Van Meerssche M.: *Nouv. J. Chim.* **1984**, *8*, 661.
6. a) Amendola V., Fabbrizzi L., Linati L., Mangano C., Pallavicini P., Pedrazzini V., Zema M.: *Chem. Eur. J.* **1999**, *5*, 3679; b) Amendola V., Fabbrizzi L., Gianelli L., Maggi C., Mangano C., Pallavicini P., Zema M.: *Inorg. Chem.* **2001**, *40*, 3579; c) Amendola V., Fabbrizzi L., Pallavicini P.: *Coord. Chem. Rev.* **2001**, *216–217*, 435; d) Amendola V., Fabbrizzi L., Pallavicini P., Sartirana E., Taglietti A.: *Inorg. Chem.* **2003**, in press.
7. Jacq J.: *J. Electroanal. Chem.* **1971**, *29*, 149.
8. a) Evans D. H.: *Chem. Rev.* **1990**, *90*, 739; b) Bard A. J., Faulkner L. R.: *Electrochemical Methods*. Wiley, New York 1980.
9. Pease A. R., Jeppesen J. O., Stoddart J. F., Luo Y., Collier C. P., Heath J. R.: *Acc. Chem. Res.* **2001**, *34*, 433.
10. Masood M. A., Enemark E. J., Stack T. D. P.: *Angew. Chem., Int. Ed. Engl.* **1998**, *37*, 928.
11. a) Baxter P. N. W., Khoury R. G., Lehn J.-M., Baum G., Fenske D.: *Chem. Eur J.* **2000**, *6*, 4140; b) Baxter P. N. W., Lehn J.-M., Rissanen K.: *J. Chem. Soc., Chem. Commun.* **1997**, 1323.
12. Low-intensity peaks are also found at higher *m/z* in the spectrum, indicating the formation of small quantities of larger oligomeric molecular cations in solution, under these conditions.

13. Molecular dynamics calculations were run with the HyperChem 3 for Windows package (Hypercube Inc. & Autodesk Inc.). The geometry optimization was performed using the MM+ force field, which is an extension of MM2, contained in the HyperChem Help Database.
14. Volume of the CH_2Cl_2 solution was 5 ml, concentration of the complex 8.0×10^{-4} mol l^{-1} and volume of each acetonitrile addition 0.1 ml. Transformation was complete after 20 additions (CH_2Cl_2/CH_3CN 5:2 v/v).
15. In this experiment, the intensity of the 416 nm band never reaches that of the fully formed one ligand/two metal complex, due to the 1:1 composition of the system.
16. Leigh D. A., Moody K., Smart J. P., Watson K. J., Slawin A. M. Z.: *Angew. Chem., Int. Ed. Engl.* **1996**, *35*, 306.
17. Sheldrick G. M.: *SADABS, Siemens Area Detector Absorption Correction Program*. University of Göttingen, Göttingen 1996.
18. Altomare A., Burla M. C., Camalli M., Cascarano G. L., Giacovazzo C., Guagliardi A., Moliterni A. G. G., Polidori G., Spagna R.: *J. Appl. Crystallogr.* **1999**, *32*, 115.
19. Sheldrick G. M.: *SHELX97, Programs for Crystal Structure Analysis*. University of Göttingen, Göttingen 1998.